Preparation and Application Research of Resin Materials Suitable for ^{90}Sr Separation in Environmental Water Samples

Si-yuan Fang, Ling Chen*, and Hai-lin Lou

Institute of Nuclear Safety and Environmental Engineering Technology, China Institute of Atomic Energy, Beijing 102413, China

Abstract. As an important fission product produced in nuclear reactors,^{90}Sr has the characteristics of high fission yield, long half-life and easy entry into the human body through the food chain. Therefore, it is a nuclide that we focus on in environmental radioactivity assessment. At present, the analysis methods for ^{90}Sr in environmental water samples generally have problems such as cumbersome pretreatment and long analysis cycles, which are difficult to meet the rapid analysis requirements for routine and emergency monitoring. To meet the rapid analysis requirements of ^{90}Sr in environmental water samples, a new type of functionalized separation resin material DtBuCH18C6@CG-71 was prepared and its separation performance in environmental water samples was investigated. The material demonstrated excellent Sr selectivity over pH 5-9, preferentially adsorbed Sr in the context of Ca, Mg, K plasma, effectively separated nuclides with significant interference of Zr, Y and Ge on ^{90}Sr mass spectrometry, with a maximum adsorption capacity of 8.9 mg/g and an adsorption equilibrium time of less than 1 min.It can maintain a recovery rate of over 92% after six regenerations, indicating that the resin has good application prospects as a separation material for ^{90}Sr mass spectrometry detection pretreatment in environmental water samples.

1 Introduction

Strontium (Sr), an alkaline earth metal present in the environment, has 27 isotopes, including four stable isotopes of ^{84}Sr,^{86}Sr, ^{87}Sr and^{88}Sr. ^{90}Sr is a typical artificial radionuclide because it has a high production (5.76%) in nuclear fission reactions [1-3]. It is a nuclide that is produced in large quantities and released into the environment during nuclear accidents, nuclear tests, and spent fuel reprocessing, and has a long physical half-life (28.90y) and biological half-cycle (7y) [4-6], making it a key radioactive nuclide in environmental radioactive monitoring.

In order to achieve precise measurement of ^{90}Sr content in environmental water samples, efficient chemical separation processes must be adopted to eliminate the interference caused by complex matrices [7]. Therefore, it is particularly important to develop a variety of chemical separation techniques for the enrichment and separation of ^{90}Sr. Since Dr. Pedersen accidentally synthesized the crown ether in 1967 while conducting research on olefin catalysts [8], researchers have systematically explored this compound. The research found that the crown ether molecule has a unique hole-like configuration. Among the many crown ethers, 18-crown-6 (18C6) and its derivatives show great potential for application in the field of separation of radionuclides ^{90}Sr because their cavity sizes are highly matched with Sr^{2+} and they can selectively coordinate with Sr^{2+} to form stable complexes. However, 18C6 is highly soluble in the aqueous phase, making it difficult to be directly used as an extractant. To improve its hydrophobicity and enhance selective recognition of Sr^{2+}, researchers introduced two cyclohexyl and two tert-butyl groups into the ring structure of 18C6, and finally synthesized di-tert-butyldi-cyclohexyl-18-crown-6 (DtBuCH18C6), molecular structure as shown in Figure 1 below. The modified crown ether is now widely used in the separation of Sr.

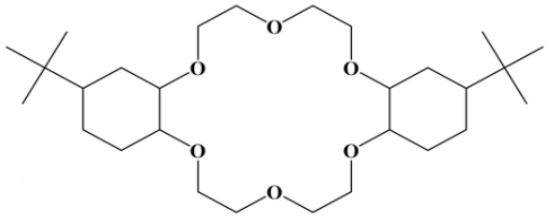

Fig. 1. Molecular structure diagram of DtBuCH18C6

To address the shortcomings of pure organic adsorbents, such as volume shrinkage during adsorption-desorption, weak radiation resistance, and low mechanical strength, DtBuCH18C6 can be loaded or grafted into organic adsorption materials to prepare adsorption resins that are resistant to solvent loss and easy to recover. The material is capable of efficiently adsorbing the radionuclide ^{90}Sr and avoiding the loss of crown ether, which has become a research hotspot for scientists in recent years.

In response to the demand for rapid analysis of ^{90}Sr in environmental water samples, separation materials that can rapidly and selectively adsorb Sr in environmental

* Corresponding author: 1182783495@qq.com

water medium are needed. Currently, commercial Sr resins generally have disadvantages such as insufficient adsorption capacity, inability to handle a large number of environmental samples simultaneously, insufficient rapid and controllable adsorption kinetics resulting in long separation time and high cost. A new type of functionalized resin was developed in this study to prepare DtBuCH18C6@CG-71 resin by immobilizing crown ether (DtBuCH18C6) onto the resin matrix. Crown ether, with its unique cavity structure, achieves size-selective recognition of Sr^{2+} and has good adsorption capacity and adsorption kinetics performance. The resin material is particularly suitable for the separation and enrichment of Sr in environmental water samples. Its surface functional groups still show high selectivity for Sr in the presence of coexisting ions such as Ca^{2+} and Mg^{2+}, and the operating conditions are relatively mild. It shows good performance in pH 5-9 and can be directly used for the treatment of environmental water samples without excessive pretreatment to adjust the water quality.

2 Instruments and reagents

Sartorius BS110S electronic analytical balance; S10-3 constant-temperature magnetic stirrer, Shanghai Sile Instrument Co., LTD.; The N-1210B rotary evaporator, Shanghai Ailang Instrument Co., LTD; TDZ5-WS low-speed centrifuge, Changsha Pingfan Instrument & Meter Co., LTD.; BT101S-V3 peristaltic pump, Baoding Leifu Fluid Technology Co., LTD.; Milli-Q ultrapure water system preparation and DKL410C constant temperature oven, German Chemical Technology (Shanghai) Co., LTD.

DtBuCH18C6 90.0%, Shanghai Maclin Biochemical Technology Co., LTD. CG-71 resin 100-150 μm, Beijing Bailingwei Ultrafine Materials Co., LTD. Anhydrous methanol, anhydrous ethanol, mesoporous SiO_2.

3 Experimental Methods

3.1 Synthesis of DtBuCH18C6@CG-71

The DtBuCH18C6@CG-71 resin was synthesized by vacuum impregnation, in which the matrix CG-71 resin was pre-treated first by mixing 300 mL of methanol with 30.0 g of the CG-71 matrix and shaking at room temperature for 24 hours to thoroughly clean its internal pore structure. Then filtration was carried out, followed by repeated rinsing with deionized water. After that, mix the matrix again with 300 mL of water and shake for 24 hours. Repeat this step more than three times to thoroughly clean and expand the pore volume of the resin, which is conducive to the subsequent impregnation of the extractant.

After the matrix cleaning is completed, take 5.0g of the treated CG-71 matrix, add 2.5g of 1 mol/L DtBuCH18C6 solution dissolved in ethanol, and add an additional 300 mL of ethanol as a dispersant to the system to ensure that the resin matrix and the extractant can be fully and evenly mixed. The mixture was then left to shake continuously at room temperature for 24 hours to ensure that the impregnation reaction was thorough and uniform. After the impregnation process was completed, the residual solvent was removed by rotary evaporation so that DtBuCH18C6 could be stably loaded onto the surface and pore structure of the CG-71 substrate. The obtained samples were then dried in a vacuum oven at 50 ℃ for 12 hours to complete the preparation.

3.2 Characterization of resin properties

To ensure that the prepared resin material has excellent performance when separating ^{90}Sr from environmental water samples, a variety of characterization methods were comprehensively employed to systematically characterize the structural characteristics and microscopic morphology of the material, providing a reliable basis for the design optimization and practical application of the material.

The surface morphology and microstructure of the material were characterized using the LE-HB08 Phenom Pro scanning electron microscope (SEM), which clearly presented the particle size, pore distribution and surface uniformity of the material surface [9]. Infrared spectroscopy analysis of the samples was performed using Thermo Nicolet NEXUS 670 Fourier transform infrared spectrometer (Thermo Nicolet Corporation, USA), and the samples were prepared by KBr pellet technique. The samples were scanned over a wavenumber range of 4000 to 400cm-1 with a resolution of 2cm-1. NMR analysis of the material was performed using the 600MHz wide-cavity solid-state NMR spectrometer of AVANCE NEO 600 MHZ WB FT-NMR, which provides high-resolution NMR spectra to ensure accurate analysis of the molecular structure of the sample.

3.3 Static adsorption test

Accurately weigh a predetermined mass of resin material and place it in a 10 mL plastic centrifuge tube. A fixed amount of solution with a pre-set acidity and a known concentration of the target ion was added to the centrifuge tube to keep the solid-liquid mass ratio stable during the adsorption experiment. Use nitric acid (HNO_3) to adjust the acidity of the solution system. Place the centrifuge tubes containing the mixed samples in a constant temperature shaker, set different temperature conditions according to the experimental design, and ensure that the adsorption reaction reaches equilibrium by shaking continuously for 24 hours. After adsorption equilibrium, remove the centrifuge tubes and centrifuge at 10,000 r/min for 5 minutes to achieve solid-liquid separation. Take a portion of the supernatant, filter it through a membrane and dilute it appropriately, and set it aside for subsequent detection and analysis. The adsorption rate R%, adsorption capacity Q_e and partition coefficient K_d are calculated as shown in Equation 1-3, where C_0 and C_t(mg/L) are the initial and post-adsorption strontium concentrations of the adsorption system, and V(L) is the volume of the solution in the adsorption system.

$$R = \frac{C_0 - C_t}{C_0} \times 100\% \quad (1)$$

$$Q_e = (C_0 - C_t) \times V \quad (2)$$

$$K_d = \frac{C_0 - C_t}{C_t} \times \frac{V}{m} \quad (3)$$

3.4 Dynamic adsorption test

The dynamic column adsorption experiment simulates the flow conditions of an actual water body by loading resin packing into the adsorption column, precisely controlling the sample to pass through the column at a specific flow rate with the help of a peristaltic pump, and determining the Sr content in the effluent, eluent, and eluent to determine the adsorption efficiency [10]. In the experiment, the adsorption performance of the material under different conditions was systematically evaluated by adjusting parameters such as flow rate, injection volume and initial concentration. The flow rate was set with reference to the actual flow of natural water bodies, while also taking into account the actual operational requirements of high-flow treatment, and the relevant parameters were reasonably optimized to enhance the representativeness and applicability of the experimental results.

4 Results and Discussion

4.1 Material characterization results

Figure 2 shows the morphologies of CG-71 and DtBuCH18C6@CG-71 resins. It can be clearly seen from the image that the untreated CG-71 resin usually presents a very regular spherical shape with a smooth surface. On the contrary, DtBuCH18C6@CG-71 the surface of the resin is covered with a thin and uniform coating. The reason for this morphological change may be that when the CG-71 resin is pretreated with methanol, both the surface and pores of the CG-71 resin are activated, and this activation process enhances the effectiveness of DtBuCH18C6 vacuum impregnation, ensuring that the adsorption activity of the DtBuCH18C6@CG-71 resin can be maintained continuously.

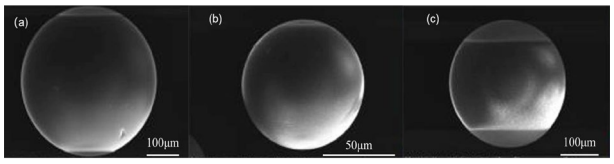

Fig. 2. Scanning electron microscopy images of DtBuCH18C6@CG-71 resin (a), CG-71 matrix (b), and DtBuCH18C6@CG-71 resin (c) after adsorbing Sr

FT-IR spectra of CG-71 resin and DtBuCH18C6@CG-71 resin are shown in Figure 3. CG-71 resin, DtBuCH18C6 and DtBuCH18C6@CG-71 resin all show specific absorption peaks. Among them, the absorption peaks at 3050 cm^{-1}, 1740 cm^{-1} and 1200 cm^{-1} represent the aromatic C-H stretching vibration, C=C stretching vibration and C-C stretching vibration respectively, which were observed in CG-71 resin and its derivative DtBuCH18C6@CG-71 resin, It indicates that the matrix structure of the resin remained intact during the synthesis process. In addition, the DtBuCH18C6@CG-71 resin also exhibits additional characteristic absorption peaks such as 2950 cm^{-1}, 2800 cm^{-1}, 1475 cm^{-1}, 1250 cm^{-1} and 1100 cm^{-1}, These absorption peaks are attributed to C-H stretching and bending vibrations, C-C stretching vibrations and C-O stretching vibrations on the DtBuCH18C6 cyclohexane and tert-butyl structures, further confirming the successful introduction of DtBuCH18C6 into the CG-71 matrix. These significant characteristic peaks not only confirm the introduction of DtBuCH18C6 into the CG-71 matrix through effective impregnation, but also indicate the uniform distribution of DtBuCH18C6 molecules within the CG-71 matrix. Furthermore, these results suggest that no chemical bonds were formed between DtBuCH18C6 and CG-71, and that the main interaction was formed by physical vacuum impregnation.

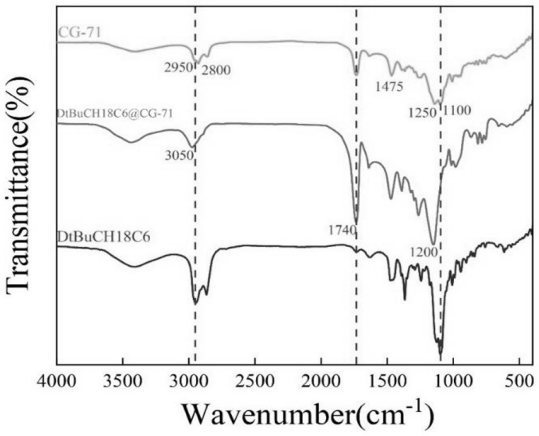

Fig. 3. FT-IR profile of DtBuCH18C6@CG-71 resin

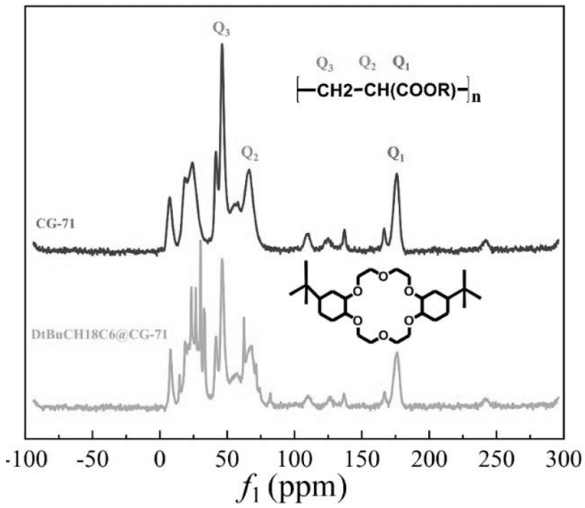

Fig. 4. ^{13}C NMR spectra of DtBuCH18C6@CG-71 resin

The ^{13}C NMR spectrum of DtBuCH18C6@CG-71 resin, as shown in Figure 4, shows a high degree of similarity to CG-71. In the spectrum, peaks at 175.6 ppm (Q_1), 65.8 ppm (Q_2), and 45.4 ppm (Q_3) represent carboxylic acid groups, -CH_2- groups, and -CH_3 groups on the surface of CG-71. The presence of these peaks reveals that DtBuCH18C6 binds to CG-71 mainly through physical adsorption rather than chemical bonds.

Compared with CG-71, the Q_1, Q_2, and Q_3 peaks of DtBuCH18C6@CG-71 resin were reduced in intensity, suggesting that DtBuCH18C6 may mask the organic functional groups on the surface of CG-71. Peaks at 22.9 ppm, 26.7 ppm, 30.7 ppm, and 32.6 ppm belong to crown ether epoxy carbon, crown ether methyl carbon, crown ether ethyl carbon, and crown ether methylene carbon. The presence of these characteristic peaks confirms that DtBuCH18C6 has been successfully loaded onto the surface and pores of CG-71 resin.

4.2 Static adsorption properties of synthetic resins

The effect of solution pH on the adsorption of Sr by synthetic resin as shown in Figure 5, the adsorption efficiency of Sr by DtBuCH18C6@CG-71 resin shows significant characteristics in different pH environments. In an acidic environment (pH 1-3), the high concentration of H^+ in the solution may inhibit the adsorption of Sr [11], at which point the adsorption rate is lower. When pH > 4, DtBuCH18C6@CG-71 shows a relatively stable adsorption efficiency over the entire pH range, especially when ph 5-9, it shows an Sr adsorption rate close to 100%. The selective adsorption effect of the resin material on Sr^{2+} is obvious, but the overall adsorption effect is poor in the highly acidic environment of pH 1-3. It is indicated that the resin is more suitable for direct use in the treatment of environmental water samples without the need for pretreatment processes such as pH adjustment of the samples.

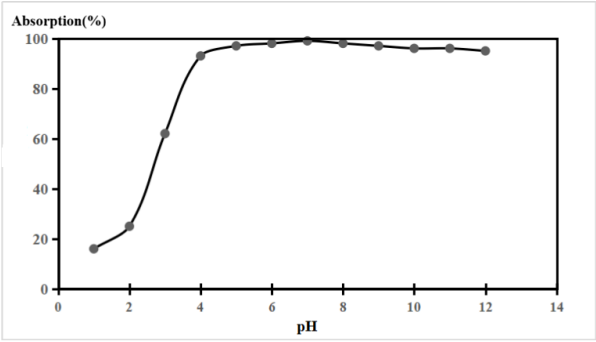

Fig. 5. Effect of pH on the Sr adsorption rate of DtBuCH18C6@CG-71 resin

To further analyze the characteristics and reaction mechanism of Sr adsorption in DtBuCH18C6@CG-71 resin materials, the thermodynamic data obtained from the experiment were analyzed using the Langmuir isothermal model, whose formula is as shown in Equation 4-6, where q_e represents the mass of Sr adsorbed per unit mass of the adsorbent at equilibrium. q_{max} represents the maximum adsorption capacity when the adsorption site reaches saturation, K_L is the Langmuir constant, which reflects the binding capacity between the adsorbate and the adsorbent, C_e represents the residual concentration of Sr when adsorption equilibrium is reached, and R_L is the Langmuir separation coefficient, which can be used to determine the favorable degree [12] of interaction between the adsorbent and the adsorbate during the adsorption process.

$$q_e = \frac{q_{max} K_L C_e}{1 + K_L C_e} \quad (4)$$

$$\frac{C_e}{q_e} = \frac{1}{K_L q_{max}} + \frac{C_e}{q_{max}} \quad (5)$$

$$R_L = \frac{1}{1 + K_L C_0} \quad (6)$$

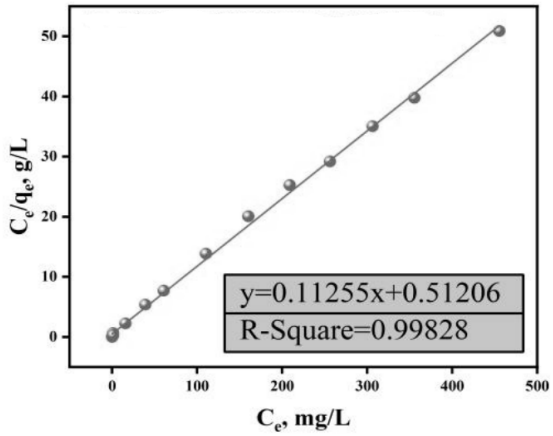

Fig. 6. Langmuir fitting results of the adsorption process of DtBuCH18C6@CG-71 resin samples

The treatment results are shown in Figure 6. When plotting C_e against C_e/q_e, the DtBuCH18C6@CG-71 resin demonstrated a high degree of conformity to the Langmuir isothermal model, with R^2=0.99828. According to Formula 5, the slope of this graph is $1/q_{max}$, from which it can be concluded that the theoretical maximum adsorption capacity of the resin for Sr(q_{max})can reach 8.9 mg/g, which is also in good agreement with the experimental data, demonstrating that the resin has a large number of available adsorption sites and excellent performance.

The adsorption kinetics data of DtBuCH18C6@CG-71 resin were fitted to explore the relationship of adsorption capacity q_e with time, and the results are shown in Figure 7 below. In the initial stage of the adsorption process, the adsorption capacity rose rapidly within just 1 minute and quickly approached the saturation adsorption level, indicating that the material has an extremely fast adsorption rate and can reach adsorption equilibrium within 1 minute, which has a significant advantage in the rapid treatment of environmental water samples. At the same time, the secondary kinetic fitting results showed a highly linear distribution, R^2=0.99992, indicating that the process of the resin adsorbing Sr was in line with the secondary kinetic model. In this model, the reaction rate is not only affected by the Sr concentration, but also closely related [13-14] to the number of active coordination sites on the resin surface and the chemical bonds formed by the adsorbent-adsorbate. From this, it is inferred that there are abundant coordination sites on the surface of DtBuCH18C6@CG-71 resin, which may chemically interact with Sr or form a strong chemical bond configuration.

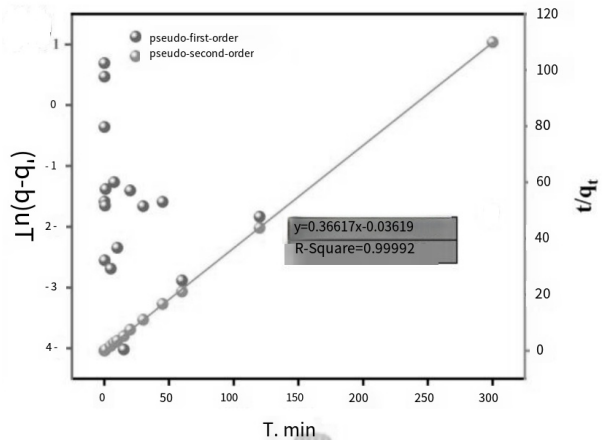

Fig. 7. Kinetic fitting results of the adsorption process of DtBuCH18C6@CG-71 resin samples

4.3 Dynamic column performance of synthetic resin

Considering the difficulty of mass spectrometry analysis of ^{90}Sr in real environmental samples, there will be multiple isomers that can cause significant interference to its analysis. The three most common interfering nuclide ions or molecular ions with m/z=90 are $^{90}Zr^{+}$,$^{90}Y^{+}$, and $^{74}Ge^{16}O^{+}$. Dynamic column flow was used to process the three interfering elements to verify the feasibility of applying the material to the pretreatment step of ^{90}Sr mass spectrometry measurement in environmental water samples. The elution curves are shown in Figure 8 below.

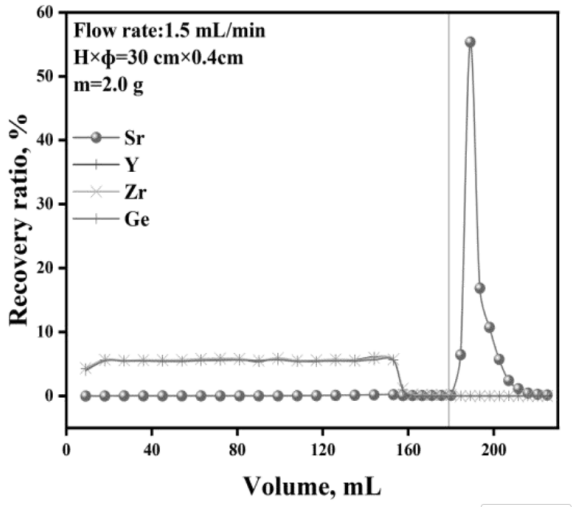

Fig. 8. Elution curves of Sr, Y, Zr, Ge from dynamic elution of a DtBuCH18C6@CG-71 resin column

At an elution volume of approximately 200 mL, the elution curve of Sr shows a sharp peak shape, indicating that under the set conditions, the DtBuCH18C6@CG-71 synthetic resin column can efficiently enrich and concentrate the elution of Sr. In this elution range, the adsorption rate of Sr rapidly increases to full loading on the column and is then rapidly eluted in a very small elution volume, reflecting the extremely high adsorption and elution efficiency of the DtBuCH18C6@CG-71 resin material. In contrast, the elution rates of Zr, Y, and Ge remained close to zero throughout the dynamic separation process, with no significant elution peaks. Under the set elution environment, the DtBuCH18C6@CG-71 resin had a weak adsorption capacity for these interfering elements, causing them to penetrate rapidly early in the dynamic column experiment. Further illustrate that the DtBuCH18C6@CG-71 resin material has a high selectivity for Sr, and the separation effect between the sample treated with the resin column and the main interfering elements is obvious.

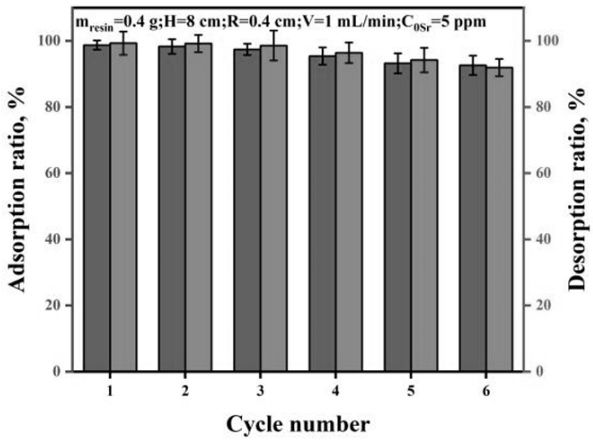

Fig. 9. The influence of the circulation times of DtBuCH18C6@CG-71 resin on the adsorption and desorption rate of Sr

To evaluate the reusability of the DtBuCH18C6@CG-71 resin material in practical applications, cyclic adsorption-desorption column experiments were conducted under simulated tap water conditions to examine its performance stability. The experimental results are shown in Figure 9. During the initial cycle stage, the adsorption efficiency of Sr by the DtBuCH18C6@CG-71 resin was almost 100%, demonstrating outstanding initial adsorption performance. As the number of cycles increased, the performance of the resin slightly declined, but it consistently maintained a recovery rate above 92%, these minor performance losses may be attributed to the following reasons: competitive ions such as Ca^{2+}, Mg^{2+}, and K^{+} in the water sample gradually occupy some of the active sites on the resin surface, causing the adsorption sites to lose their activity; physical swelling of the resin material caused by the eluent; and some Sr^{2+} forms a relatively strong irreversible chemical adsorption with the resin, which is difficult to desorb and regenerate under conventional conditions. Despite these minor performance losses, the DtBuCH18C6@CG-71 resin still demonstrates excellent recyclability and has promising application prospects.

5 Conclusion and Prospect

To meet the demand for rapid analysis of ^{90}Sr in environmental water samples, a novel functionalized resin, DtBuCH18C6@CG-71, was developed. This material was synthesized using vacuum impregnation technology, with CG-71 resin as the matrix and DtBuCH18C6 functionalized extractant effectively immobilized.

Through systematic characterization, static adsorption, dynamic column experiments, thermodynamic and kinetic fitting, and other experiments, the comprehensive performance of the composite material was systematically evaluated and confirmed. It was demonstrated that the DtBuCH18C6@CG-71 composite material can efficiently remove complex interfering components in environmental water samples, enabling selective separation and enrichment of Sr elements without excessive pretreatment. As a separation material for the pretreatment of ^{90}Sr mass spectrometry detection in environmental water samples, it shows good application prospects.

At present, although some progress has been made in the separation technology of ^{90}Sr in environmental water samples, there are still many difficult problems that need to be further studied and optimized. For instance, the current work is mainly based on laboratory simulation conditions and is limited to small and medium-scale sample volumes. More systematic validation work on real environmental samples needs to be carried out, including surface water, groundwater, and seawater under different geological conditions, to establish a complete application database. Additionally, by optimizing the microstructure design of the material, regulating its pore size distribution and surface chemical properties, the material's tolerance to extreme environments and resistance to salt interference can be further enhanced, making it suitable for more complex environmental matrices such as soil and biological samples. Moreover, for the practical operation problems that may occur in the processing of large-volume and large-batch samples, such as resin bed clogging and unstable flow rate, the column design and operation parameters need to be optimized.

References

1. Cui Q., Lu J., Li X., et al. A ^{90}Sr / ^{90}Y -radioisotope battery based on betavoltaic and beta-photovoltaic dual effects[J]. Materials Science in Semiconductor Processing, 2024,179: 108493.
2. Sun S., Yang M., Wang N.,et al. Enhanced adsorption dynamics and thermal stability of radioactive Sr(II) by lamellar Nb-doped sodium vanadosilicate via self-assembly and conditional natroxalate intercalation[J]. Journal of Hazardous Materials, 2024, 471:134431.
3. Klingelhoefer D., Braun M.,Gerhard M. OremekDoerthe BrüggmannDavid A. Groneberg. Global research on nuclear energy in the context of health and environmental risks, considering economic interests[J]. Wiley interdisciplinary reviews. Energy and environment, 2024, 13(1):e497.1-e497.17.
4. Zu J., Diao J., Han G., et al. Highly efficient and selective removal of ^{90}Sr by the carboxylated COFs (Tp-DTA) from radionuclides-contaminated groundwater[J]. Separation and Purification Technology, 2024, 338(000):12.
5. Singh R., Prasad B., Ahn Y. H. Recent developments in gas separation membranes enhancing the performance of oxygen and nitrogen separation: A comprehensive review[J].Gas Science and Engineering, 2024, 123(000).
6. Wei Y., Cao L., Zhu J., et al. Radioactive strontium ions sieving through reduced graphene oxide membrane[J].Journal of Membrane Science, 2024, 689
7. Kavasi N., Arae H., Aono T., et al. Distribution of strontium-90 in soils affected by Fukushima dai-ichi nuclear power station accident in the context of cesium-137 contamination[J].Environmental Pollution, 2023,326:121487.
8. Pedersen C. J. Cyclic Polyethers and Their Complexes With Metal Salts[J].Journal of the American Chemical Society, 1967, 89(26):7017-7036.
9. Joseph I. G. Scanning Electron Microscopy and X-Ray Microanalysis 4th Edition[M]. Springer,2017.
10. Nesterenko P. N. Ion chromatography [M]. Liquid Chromatography. Elsevier. 2023: 465-507.
11. Su Y., He J., Liu X. Conveniently synthesis of porous crown-based resin with efficient ~(90)Sr capture from highly acidic wastewater[J].Separation and Purification Technology, 2024:334:126051.
12. Fomkin A. A. Adsorption of Gases, Vapors and Liquids by Microporous Adsorbents[J].Adsorption-journal of the International Adsorption Society, 2005, 11(3-4):425-436.
13. Wu F. C., Tseng R. L., Huang S. C., et al. Characteristics of pseudo-second-order kinetic model for liquid-phase adsorption: A mini-review[J]. Chemical Engineering Journal, 2009, 151(1-3):1-9.
14. Qiu H., Lv L., Pan B. C., et al. Critical review in adsorption kinetic models[J].Journal of Zhejiang University-SCIENCE A, 2009(05):716-724.